

Cutoff wave number for shear waves and Maxwell relaxation time in Yukawa liquids

J. Goree

Department of Physics and Astronomy, The University of Iowa, Iowa City, Iowa 52242, USA

Z. Donkó and P. Hartmann

Research Institute for Solid State Physics and Optics of the Hungarian Academy of Sciences, P. O. Box 49, H-1525 Budapest, Hungary

(Received 12 December 2011; published 11 June 2012)

Because liquids cannot resist shear except over very short distances comparable to the atomic spacing, shear sound waves (i.e., transverse phonons) propagate only for very short wavelengths. A measure of this limit is the cutoff wave number k_c , which is sometimes called the critical wave number. Previously k_c was determined in molecular dynamics (MD) simulations by obtaining the dispersion relation. Another approach is developed in this paper by identifying the wave number at the onset of a negative peak in the transverse current correlation function. This method is demonstrated using a three-dimensional MD simulation of a Yukawa fluid, which mimics dusty plasmas. In general, k_c is an indicator of conditions where elastic and dissipative effects are approximately balanced. Additionally, the crossover frequency for the real and imaginary terms of the complex viscosity of a dusty plasma is obtained; this crossover frequency corresponds to the Maxwell relaxation time.

DOI: [10.1103/PhysRevE.85.066401](https://doi.org/10.1103/PhysRevE.85.066401)

PACS number(s): 52.27.Gr, 52.27.Lw, 61.20.Lc, 83.60.Bc

I. INTRODUCTION

Solids, unlike gases, can sustain two kinds of sound waves (phonons): compressional and transverse. The compressional wave is longitudinal, like a sound wave in air, with a periodic compression and rarefaction and wave propagation in a direction parallel to the collective particle velocities. The transverse wave has shear motion, with wave propagation perpendicular to collective particle velocities. The ability of a medium to sustain a shear wave requires an elastic response to a disturbance, where a particle tends to be restored to its equilibrium position after being disturbed.

A liquid, unlike a solid, exhibits elastic responses only for a limited time and over a limited distance. This is so because the potential landscape surrounding a particle in a liquid does not remain unchanged indefinitely as in a solid. When neighboring particles rearrange their positions irreversibly, there will also be an irreversible change in the confining potential landscape, and energy will be dissipated. Until a rearrangement occurs, a disturbance in the position of one particle can be restored elastically.

One approach used in the theory of liquids for characterizing the conditions for elastic vs dissipative motion is based on the propagation of the shear wave. Shear waves with a wave number less than a minimum wave number k_c cannot propagate [1]. Theoretical authors have referred to this minimum wave number as a “critical wave number” or a “cutoff wave number,” and we will adopt the latter term. Typically k_c has a value of $k_c a \approx 1$, within a factor of 3, depending on temperature and other parameters of the liquid. Here, a is a measure of interparticle distances in a liquid, defined as the Wigner-Seitz radius $a = (3/4\pi n)^{1/3}$ for a number density n .

The cutoff wave number has practical importance not only in simple liquids, but also in strongly coupled plasmas like those that we study here, and in supercooled liquids [2]. The cutoff wave number has been observed identified in molecular dynamics (MD) simulations including [3–5] for three-dimensional (3D) liquids and [6] for 2D liquids. A direct observation of the cutoff wave number has been made, to

our knowledge, in one experiment [7], which used a dusty plasma. A dusty plasma is an ionized gas containing charged particles of solid matter [8–10]. Dusty plasma experiments have also been reported to characterize static viscosity [11] and viscoelastic effects [12,13].

Previous methods of determining k_c include examining a dispersion relation ω vs k of the shear waves. By tracking particle positions and velocities in an MD simulation, one can compute a phonon spectrum, i.e., a graph of wave energy as a function of ω and k . In such a graph, energy is concentrated in a band in ω - k space. Drawing a curve along the peaks of this band yields the dispersion relation. For a liquid, this dispersion relation curve does not extend down to $\omega = 0$ and $k = 0$ as it does for a solid, but instead ends at an intercept on the $\omega = 0$ axis. The previous method of determining $k = k_c$ is by extrapolating the observed dispersion relation curve to this intercept, as has been done for liquids in three [5] and two dimensions [14]. We present in Fig. 1 an example of such a dispersion relation, as determined from the 3D MD simulation reported in this paper. The simulation method and parameters are described in Sec. II.

In this paper, we develop another quantitative method to determine the cutoff wave number k_c . This method is based on identifying a negative peak in a correlation function and extrapolating to the condition where this peak vanishes. We present this method and demonstrate its usefulness over a wide range of temperature using MD simulation data for a liquid strongly coupled plasma in Sec. III D.

A strongly coupled plasma is a collection of free charges that have an interparticle potential energy that is greater than the thermal kinetic energy. Such a strongly coupled plasma can have the structure of a solid or a liquid, depending on whether the temperature is below or above a melting point [15]. It is common to describe a strongly coupled plasma by the dimensionless Coulomb coupling parameter

$$\Gamma = \frac{Q^2}{4\pi\epsilon_0 a k_B T}, \quad (1)$$

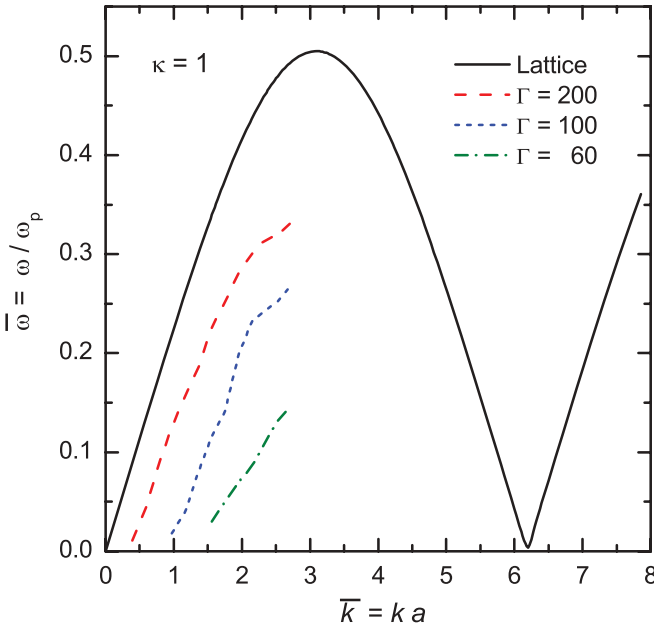


FIG. 1. (Color online) Example of dispersion relations of shear waves in a 3D Yukawa liquid. The curves for the dispersion relations were determined as the peaks of the phonon spectrum computed using our MD simulation, which is a method used by previous authors, e.g., [4]. Note the absence of a dispersion relation for very small wave numbers: this indicates the cutoff k_c . Also shown for comparison is the dispersion relation for propagation along a primitive vector of a bcc lattice for the same κ . The quantities shown are dimensionless; the wave number is normalized $\bar{k} = ka$ where a is the Wigner-Seitz radius, and the frequency is normalized $\bar{\omega} = \omega/\omega_p$ where ω_p is the plasma frequency.

where Q is the charge of the particles and T is the temperature. When Debye screening occurs, the electric potential of a point charge can be described as the Yukawa (Debye-Hückel) potential energy $\phi = (Q^2/4\pi\epsilon_0 r) \exp(-r/\lambda)$, where λ is a screening length. In this case, another dimensionless parameter is the screening parameter

$$\kappa = a/\lambda. \quad (2)$$

Time scales in a strongly coupled plasma are characterized by the plasma frequency

$$\omega_p = (nQ^2/\epsilon_0 m)^{1/2}, \quad (3)$$

where m is the mass of a particle.

We will use the Yukawa potential, which is used often to describe dusty plasmas [16] as well as charged colloidal suspensions. A Yukawa system can behave as a liquid, as has been studied in both simulations and experiments, of which we will mention a few. The melting point of a 3D Yukawa system has been determined in MD simulations [17] to be $\Gamma_{\text{melt}} = 217.4, 440.1, \text{ and } 1185$ for $\kappa = 1, 2, \text{ and } 3$, respectively. The complex viscosity $\eta(\omega)$ has been characterized in 3D simulations [18] and a 2D dusty plasma experiment [19].

In addition to determining k_c , we will also use our simulation to determine the frequency-dependent viscosity of a Yukawa fluid. The frequency-dependent viscosity

$$\eta(\omega) = \eta'(\omega) - i\eta''(\omega) \quad (4)$$

is a formalism to describe two characteristics of viscoelastic effects: the real part η' indicates dissipation while the imaginary part η'' indicates elasticity, i.e., energy storage. As we will discuss in Sec. III, there is a frequency ω_{cross} for which the curves for $\eta'(\omega)$ and $\eta''(\omega)$ cross over, and the inverse of this crossover frequency is the Maxwell relaxation time τ_M . We will present results for the frequency-dependent viscosity and Maxwell relaxation time for a Yukawa fluid in Sec. III C.

II. SIMULATION

A. Method

We use the equilibrium molecular dynamic simulation method as described in [18]. To imitate an infinite liquid, the simulation has periodic boundary conditions, which is suited for studying the intrinsic properties of a substance. This differs from the approach of simulations in a bounded system [20]. In a system containing N particles, we integrate the equation of motion of a particle i ,

$$m \frac{d\mathbf{v}_i}{dt} = -Q \sum_{j \neq i}^N \nabla \phi_{ij}, \quad (5)$$

where ϕ_{ij} is the potential for a binary Yukawa interaction at the position of particle i due to particle j . We use the resulting time series data for positions and velocities of particles to calculate the transverse microscopic current

$$\tau_{xy}(k, t) = \sum_{j=1}^N v_{xj} e^{iky_j} \quad (6)$$

and the off-diagonal elements of the shear stress tensor

$$P_{xy}(t) = \sum_{i=1}^N \left[m v_{ix} v_{iy} - \frac{1}{2} \sum_{j \neq i}^N \frac{x_{ij} y_{ij}}{r_{ij}} \frac{\partial \phi(r_{ij})}{\partial r_{ij}} \right], \quad (7)$$

where $r_{ij} = |\mathbf{r}_{ij}| = |\mathbf{r}_i - \mathbf{r}_j| = |(x_{ij}, y_{ij})|$.

When we present our results in Sec. III, it will be useful to know that in Eq. (7) the first term on the right-hand side arises from kinetic effects that are dominant for liquids at high temperatures, while the second term arises from potential effects that are dominant at low temperatures [21]. These potential effects include caging [22,23] and decaging [24] of particles.

We then calculate the transverse current autocorrelation function

$$C_T(k, t) = \langle \tau_{xy}(k, t) \tau_{xy}^*(k, t) \rangle \quad (8)$$

and the shear stress autocorrelation function

$$C_\eta(t) = \langle P_{xy}(t) P_{xy}(0) \rangle. \quad (9)$$

We can use Eq. (9) in the generalized Green-Kubo relation

$$\eta(\omega) = \frac{1}{VkT} \int_0^\infty C_\eta(t) e^{i\omega t} dt \quad (10)$$

to calculate the complex viscosity, Eq. (4). Here, $V = L^3$ is the simulation volume. As in [18], we replace the upper limit in Eq. (10) with the time when the correlation function first crosses zero. Equation (10), which can be derived from expressions in [25], includes a complex exponential so that

it is a generalization of the usual Green-Kubo relation. The latter is known to predict viscosity values that agree with those obtained by hydrodynamic schemes for steady-state conditions.

B. Parameters

The simulated cell contains $N = 8000$ identical particles in a cube with sides of length $L \approx 32.24a$. This length defines a minimum resolvable wave number $2\pi/L \approx 0.195a^{-1}$. The time step is chosen as $\Delta t \leq (\pi/15)\omega_p^{-1}$. The simulation is run for an initial thermalization period of 10^5 time steps, and then data are recorded for 10^6 time steps. We repeat the simulation over a wide range of the Coulomb coupling parameter $\Gamma < \Gamma_{\text{melt}}$ and three values of the screening parameter $\kappa = 1, 2,$ and 3 .

C. Dimensionless variables

We report results that are in dimensionless units, as indicated by bars over the symbols. These are the length $\bar{r} = r/a$, wave number $\bar{k} = ka$, correlation functions $\bar{C}(t) = C(t)/C(0)$, viscosity $\bar{\eta} = \eta/mn\omega_p a^2$, and frequency $\bar{\omega} = \omega/\omega_p$. For some results we will also report frequencies normalized as ω/ω_E , where ω_E is the Einstein frequency, whose values are reported in Table I of [17]. We make time t dimensionless by multiplying by the plasma frequency $\omega_p t$. Other dimensionless variables are Γ and κ as defined in Eqs. (1) and (2), respectively.

III. RESULTS AND DISCUSSION

A. Dispersion relation

A method used by previous authors to identify a cutoff wave number is the measurement of the dispersion relation. One way of doing this is to perform an MD simulation to record the positions and velocities of particles undergoing thermal motion and use these data to compute the power spectrum in the ω - k space. The peaks of this power spectrum correspond to the wave dispersion relation.

An example of a dispersion relation is presented in Fig. 1, based on our MD simulation. The previous method of determining k_c is to extrapolate these dispersion relation curves to their intercept on the $\omega = 0$ axis.

B. Cutoff wave number: Transverse current correlation method

An example of the transverse current correlation function C_T , defined in Eq. (8), is shown in Fig. 2(a) for our simulation with $\Gamma = 125$ and $\kappa = 1$. For small wave numbers, i.e., in the hydrodynamic limit, C_T decays monotonically. For large wave numbers, C_T exhibits oscillations, which are considered as indications of the presence of shear waves [26,27]. The feature of interest to us is the first negative peak in these oscillations.

Here, we present a method of determining k_c quantitatively using this negative peak. The steps are as follows. We compute C_T for a specified value of k , and we determine the amplitude A of its largest negative peak. We repeat this for a series of four or five k values, and we plot the trend for A vs k . Fitting a straight line through these data points, as in Fig. 2(b), we extrapolate

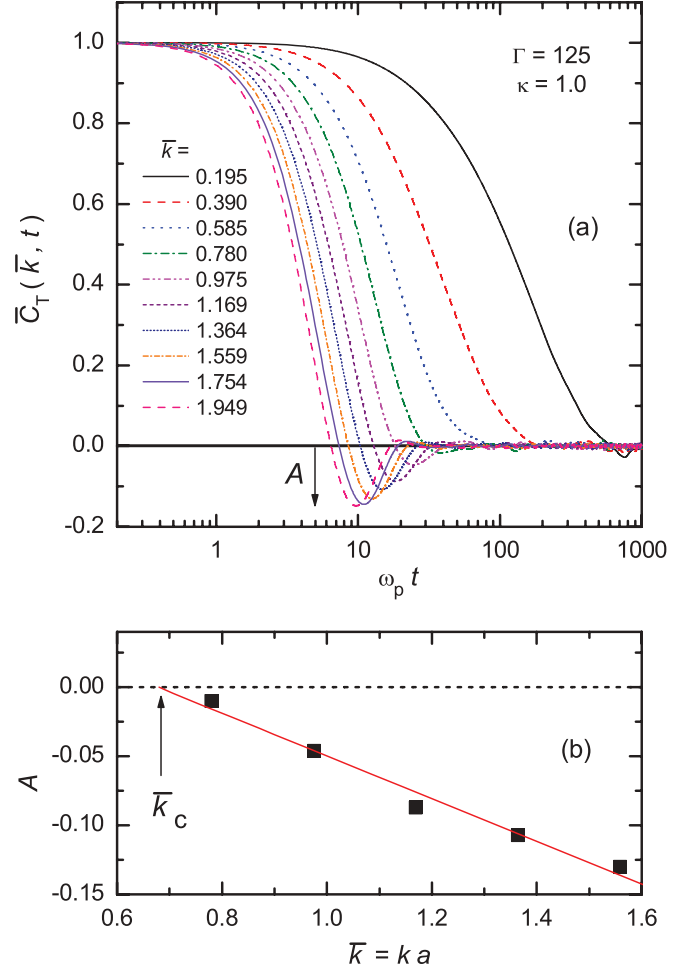


FIG. 2. (Color online) (a) Example of transverse current autocorrelation function C_T for a liquid at a temperature nearly twice as high as the melting point, for various wave numbers k . The hydrodynamic limit is at small wave numbers while at larger wave numbers there are oscillations. (b) Method of determining the cutoff wave number k_c . We measure the amplitude A of negative peaks of C_T in (a) for various values of k , and plotting these we extrapolate to find the value of k where the amplitude just touches a zero value, i.e., where the curve for C_T would barely have a negative oscillation in the absence of noise; we report this value of k as our measure of k_c . The vertical axis of (a) is normalized by the value of the correlation function at zero time, $\bar{C}(t) = C(t)/C(0)$.

to identify the value of k where the amplitude approaches zero. This extrapolated value at the onset of oscillations in C_T corresponds to the onset of shear wave propagation. We therefore report this extrapolated wave number as our measure of the cutoff wave number k_c .

Applying this method to our simulation data for a 3D Yukawa liquid, we find the cutoff wave number k_c for a liquid over a wide range of Γ . The cutoff wave number is generally in a range $0.3 \lesssim \bar{k}_c \lesssim 3$, where the smaller values of \bar{k}_c correspond to temperatures near the melting point.

We also find that, when normalized, the values for the cutoff wave number fall on a universal curve (see Fig. 3). This curve is approximately $\bar{k}_c = \frac{1}{3}(\Gamma/\Gamma_{\text{melt}})^{-4/3}$. To make the data fall on this curve, we normalized k_c by a and Γ by the melting point Γ_{melt} .

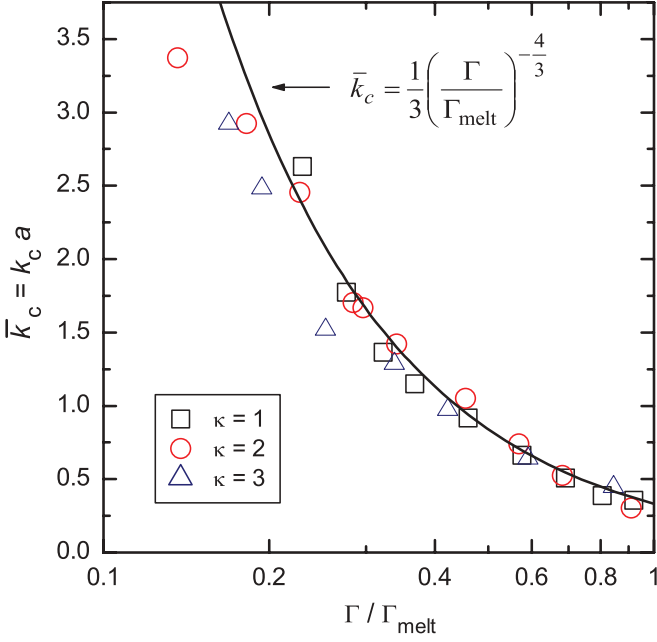


FIG. 3. (Color online) Results for cutoff wave number k_c , determined from our MD simulation, measured as in Fig. 2 by identifying the smallest value of k that would allow a negative oscillation of the transverse current correlation. Data are shown as a function of the Coulomb coupling parameter Γ , which serves as a measure of inverse temperature, and they are normalized by the melting point Γ_{melt} data from [17]. Generally k_c decreases with Γ , i.e., increases with temperature.

As a validation, we compared our results for the cutoff wave numbers to those reported by Murillo [28] and by Hamaguchi and Ohta [5]. They both determined k_c from a dispersion relation, which they obtained by different means. Murillo used a hydrodynamic method, while Hamaguchi and Ohta used an MD simulation. We find general agreement when comparing our values and theirs. This agreement is improved by dividing their values of k_c by a factor of $\sqrt{2}$, which is reasonable considering Murillo's argument that the dispersion relation methods generate a value of k_c that is larger than the true onset of waves by a factor of $\sqrt{2}$ [28]. Our method detects the onset of waves.

C. Crossover frequency: Complex viscosity method

For comparison, we present here another indicator of the balance of elastic and dissipative effects, characterized by a frequency instead of a wave number, and based on viscosity instead of waves. This is done by exploiting the frequency-dependent viscosity Eq. (4), which has a real part $\eta'(\omega)$ that corresponds to viscous dissipation, and an imaginary part $\eta''(\omega)$ that corresponds to elasticity, i.e., energy storage.

Here, we do not investigate the full dependence of η on both ω and k because our Green-Kubo method yields valid results only with $k = 0$ [25]. We also note that a dependence on only frequency is what is typically measured in experiments, for example using rheometers that agitate a liquid by rotating at a specified frequency ω . Besides our Green-Kubo method, there exist other theoretical methods that have been used

to generate the full frequency and wave-number-dependent viscosity, which we do not attempt to use [29].

In the theory of liquids, the viscoelastic approximation [30] predicts the real and imaginary parts of viscosity as

$$\eta'(\omega) = \frac{\eta}{1 + \omega^2 \tau_M^2}, \quad (11)$$

$$\eta''(\omega) = \frac{\eta \omega \tau_M}{1 + \omega^2 \tau_M^2}, \quad (12)$$

where η is the usual static viscosity for $\omega \rightarrow 0$, and τ_M is the Maxwell relaxation time [30]. The real part η' is larger at low frequencies, while the imaginary part η'' is larger at high frequencies. Inspecting Eqs. (11) and (12), we see that the real and imaginary parts are equal, i.e., their curves cross over, at $\omega = 1/\tau_M$.

This prediction for the viscoelastic approximation, a crossover of the real and imaginary terms at a physically significant frequency of $1/\tau_M$, leads us to inspect graphs of the complex viscosity from our MD simulation, produced using Eq. (10).

An example of the complex viscosity and the crossover of its real and imaginary terms is shown in Fig. 4. The data points are our simulation results. Note that the real part η' diminishes monotonically with frequency, so that its curve crosses that of the imaginary part η'' . In this example, for $\Gamma = 125$ and $\kappa = 1$, the crossover occurs at $\omega_{\text{cross}} = 0.240\omega_p$. We interpret $1/\omega_{\text{cross}} = 4.17\omega_p^{-1}$ as an empirical measure of τ_M , for the parameters of Fig. 4.

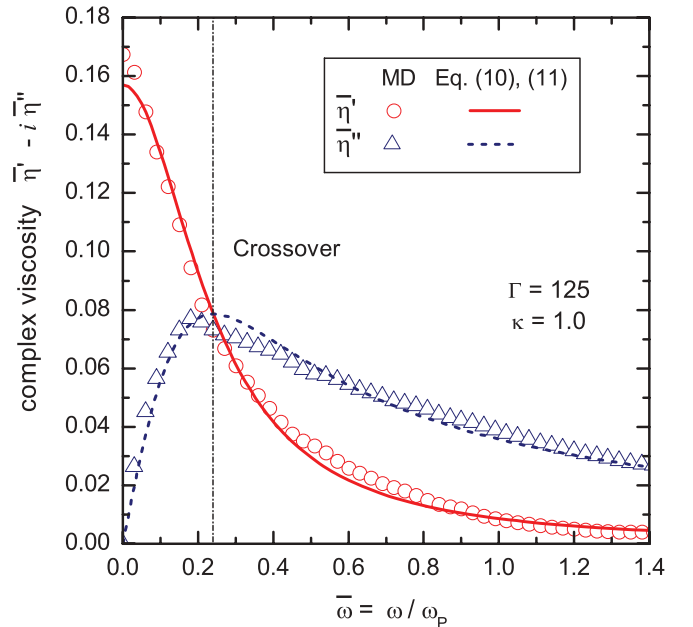


FIG. 4. (Color online) Terms of the complex viscosity, where the real term η' indicates dissipation and the imaginary term η'' indicates storage of energy. Data points are from the MD simulation. The real and imaginary terms cross over in this case at $\bar{\omega}_{\text{cross}} = 0.240$. We interpret this crossover of the real and imaginary terms as an indication of a balance of dissipation and elasticity. Also shown are curves for a fit to Eqs. (11) and (12) for the viscoelastic approximation, with fit parameters $\bar{\eta} = 0.157$ and $\tau_M = 4.152\omega_p^{-1}$. Viscosity is normalized here as $\bar{\eta} = \eta/mn\omega_p a^2$.

Also shown in Fig. 4 is a fit of our MD simulation data to the viscoelastic approximation Eqs. (11) and (12). This fit, which has only two free parameters, η and τ_M , shows good agreement. The fit yields $\tau_M = 4.15\omega_p^{-1}$, for the parameters $\Gamma = 125$ and $\kappa = 1$ of Fig. 4. The fit is good, as indicated by an agreement within 0.5% when compared to $1/\bar{\omega}_{\text{cross}}$ for the simulation data points.

We repeat this calculation of the crossover frequency ω_{cross} for a wide range of Γ and κ , and the result is shown in Fig. 5(a). By normalizing the axes differently in Fig. 5(b), as ω/ω_E vs $\Gamma/\Gamma_{\text{melt}}$, we find that the curves for various screening parameters κ are similar.

The curves for ω_{cross} in Fig. 5 have a peak. We verified that this peak nearly coincides with a minimum of viscosity. This minimum of viscosity is a well-known phenomenon for liquid strongly coupled plasmas. It occurs between low temperatures where the potential terms in Eq. (7) dominate and high temperatures where the kinetic terms dominate [21]. For the purpose of understanding viscoelasticity, only the high- Γ regime is of interest, which in Fig. 5(b) is for $\Gamma/\Gamma_{\text{melt}} \gtrsim 0.1$. In this case the viscosity is dominated by potential effects, and particles can be caged for a finite time between their nearest neighbors, as is required for elasticity. This is the same range of Γ where we found oscillations in the transverse current correlation function that indicate the presence of shear waves, as indicated in Fig. 3.

Within the regime $\Gamma/\Gamma_{\text{melt}} \gtrsim 0.1$ that is meaningful for viscoelasticity, we find a trend that the crossover frequency diminishes with increasing Γ . We can suggest an intuitive explanation for this trend. For this relatively low-temperature range, viscous effects are dominated by the second term of Eq. (7), which arises from potential energy terms that can result in caging. Consider that ω_{cross} indicates a balance of dissipative and elastic effects, and that dissipation involves the slipping of particles out of a cage. This decaging requires a displacement that is a significant fraction of the particle spacing. Since the particle has a finite velocity, characterized by the thermal velocity, this displacement requires a finite time. At a high frequency ω , there is too little time, $1/\omega$, for this to occur, and elastic effects will dominate. Only at a sufficiently low frequency $\omega < \omega_{\text{cross}}$ will there be sufficient time for a particle to slip enough to decay. As the temperature is decreased (i.e., Γ is increased), the thermal velocity is reduced and the time required for slipping becomes longer. Thus, we generally expect ω_{cross} to diminish as Γ is increased. This is the trend that is observed in our data in Fig. 5, for $0.1 < \Gamma/\Gamma_{\text{melt}} < 1$.

D. Cutoff wave number vs crossover frequency

We have developed a quantitative method of measuring the cutoff wave number determined by extrapolating a negative peak in a correlation function to the point at which it vanishes, as an indication of a balance of dissipative and elastic effects as a function of Γ . As another method of indicating a balance of dissipative and elastic effects, we also presented results for a better-known method, the complex viscosity, which has two terms that cross at a frequency that we find. We can combine these results from Figs. 3 and 5 into a single graph of ω_{cross} vs k_c , in Fig. 6.

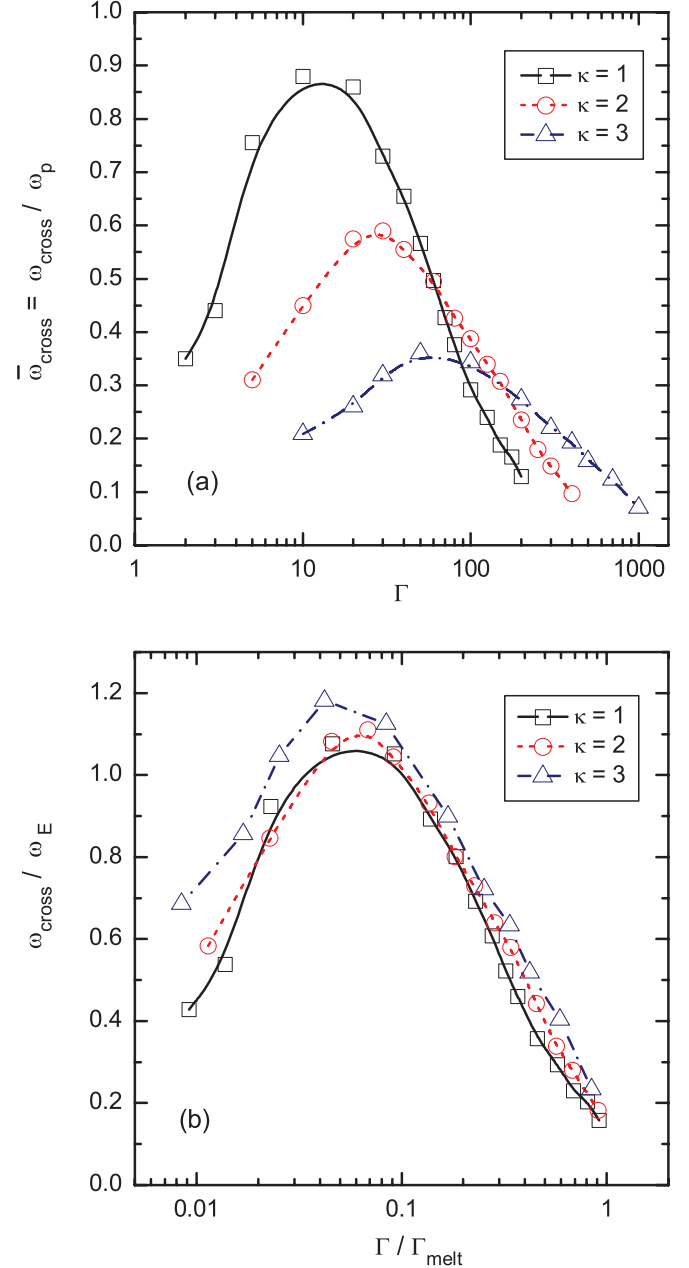


FIG. 5. (Color online) Crossover frequency ω_{cross} , determined as in Fig. 4. Results are shown in (a) in our usual dimensionless variables. In (b) the frequency is normalized by the Einstein frequency ω_E and the inverse temperature Γ is normalized by the melting point, showing a similarity. Data points to the right of the peak are meaningful for viscoelastic effects.

In Fig. 6, the data points in the lower left-hand corner are for low temperatures near the melting point, i.e., high Γ , while those in the upper right are for high temperature. Beyond the last data points in the upper right, the effects of elasticity vanish.

The significance of any given data point in Fig. 6(a) is that for its value of Γ and κ , the data point marks a frequency ω and a wave number k where elastic and dissipative effects balance. Elastic effects dominate for the parameter space k to the right and ω above the data point, while dissipative

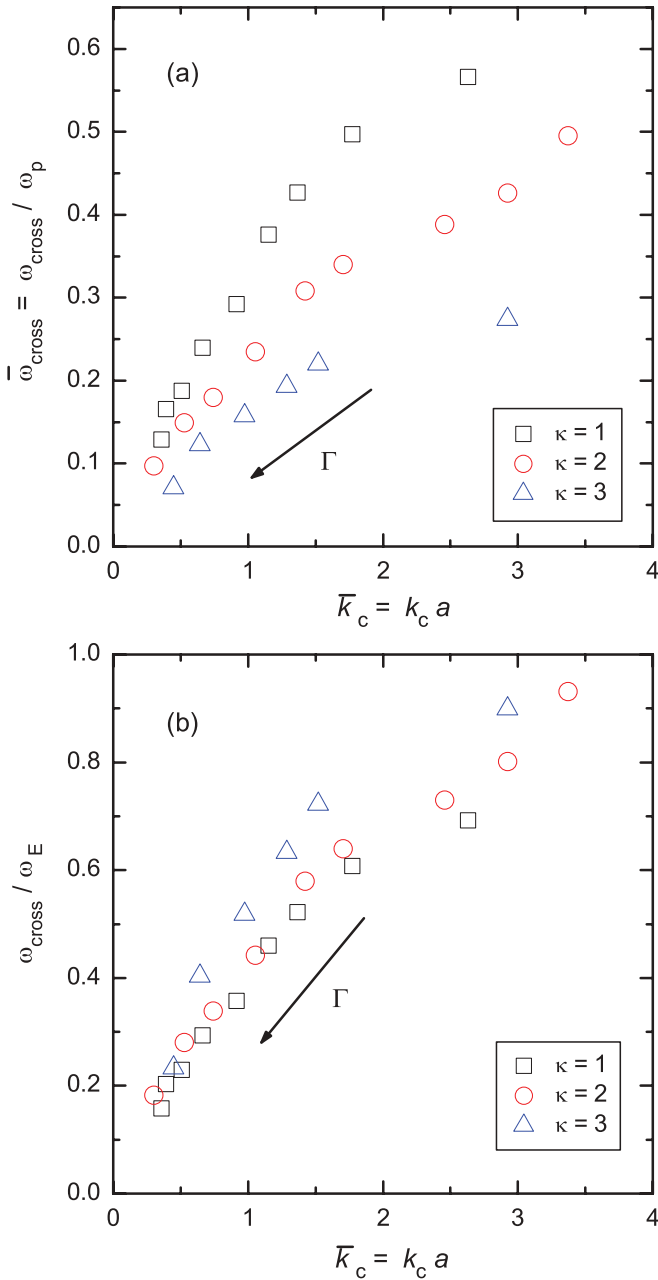


FIG. 6. (Color online) Results from Figs. 3 and 5 combined. Data for liquids are shown in (a) with our usual dimensionless units and in (b) with frequency normalized by the Einstein frequency. A crystalline solid would appear at the origin in this graph.

effects dominate to the left and below the data point. For lower temperatures, i.e., for data points nearer the origin in Fig. 6, a greater portion of the ω - k parameter space is dominated by elastic effects, as compared to higher temperatures. This temperature dependence is the reason that the data points are distributed along a curve with a distinctive trend in Fig. 6.

All the data points in Fig. 6 are for a liquid. A crystalline lattice at zero temperature would appear at the origin in this graph. This is so because dissipation is lacking and elastic effects dominate, for all values of k and ω in a perfect crystal.

To avoid confusion, we should mention that despite its appearance as a graph of a frequency vs a wave number, Fig. 6 is not a dispersion relation. The vertical axis ω_{cross} has no direct relation to waves.

IV. CONCLUSIONS

We have developed a method of determining the cutoff wave number for shear waves, by detecting the presence of an oscillation in the transverse current correlation function $C_T(t)$. This is a sensitive method of detecting the onset of shear waves, and it allows a determination of the cutoff wave number. This method is useful over a wide range of temperatures, even as hot as ten times the melting point for the 3D Yukawa liquid that we studied. We obtained the data for this test using an equilibrium MD simulation. We empirically found the temperature dependence, i.e., the dependence on the coupling parameter Γ , to be $\bar{k}_c = \frac{1}{3}(\Gamma/\Gamma_{\text{melt}})^{-4/3}$.

For comparison, we have also presented results from another method of identifying a balance of the effects of viscous dissipation and elasticity: a determination of the crossover frequency for the real and imaginary parts of the frequency-dependent complex viscosity. This method, which in principle could be useful for experiments as well as simulations, relies on the meaning of the real part of the viscosity as an indicator of dissipation and the imaginary part as an indicator of elasticity. The inverse of this crossover frequency is an empirical measure of the Maxwell relaxation time, which is a well-known parameter in viscoelastic theory that we determined for a dusty plasma.

This crossover frequency method yields results over a wide range of temperature, although for the purposes of understanding the elastic part of viscoelasticity it is likely meaningful only for the same temperature range as our cutoff wave number method. That range is the one where the potential terms dominate the viscosity, which for our 3D Yukawa liquid is roughly $0.1 < \Gamma/\Gamma_{\text{melt}} < 1$.

Note added in proof. An agreement of the Green-Kubo method and a hydrodynamic method of computing the shear viscosity was demonstrated recently for Yukawa liquids by Mithen *et al.* [31]. For the hydrodynamic limit, they also confirmed the monotonic decay of the transverse current autocorrelation function C_T for a Yukawa liquid.

ACKNOWLEDGMENTS

This work has been supported by the Hungarian Fund for Scientific Research through Grants No. OTKA-K77653, PD75113, and NN103150. Work in the USA was supported by the National Science Foundation and NASA.

[1] P. A. Egelstaff, *An Introduction to the Liquid State*, 2nd ed. (Oxford University Press, Oxford, 1994).
 [2] S. P. Das, *Phys. Rev. E* **62**, 1670 (2000).

[3] D. Levesque, L. Verlet, and J. Kürkijarvi, *Phys. Rev. A* **7**, 1690 (1973).
 [4] H. Ohta and S. Hamaguchi, *Phys. Rev. Lett.* **84**, 6026 (2000).

- [5] S. Hamaguchi and H. Ohta, *Phys. Scr. T* **89**, 127 (2001).
- [6] Lu-Jing Hou, Z. L. Miškovic, A. Piel, and M. S. Murillo, *Phys. Rev. E* **79**, 046412 (2009).
- [7] V. Nosenko, J. Goree, and A. Piel, *Phys. Rev. Lett.* **97**, 115001 (2006).
- [8] P. K. Shukla and A. A. Mamun, *Introduction to Dusty Plasma Physics* (Institute of Physics Publishing, Bristol, 2002).
- [9] G. E. Morfill and A. V. Ivlev, *Rev. Mod. Phys.* **81**, 1353 (2009).
- [10] *Introduction to Complex Plasmas*, edited by M. Bonitz, N. Horing, and P. Ludwig, Springer Series on Atomic, Optical, and Plasma Physics (Springer, New York, 2010).
- [11] O. S. Vaulina *et al.*, *Phys. Lett. A* **372**, 1096 (2008).
- [12] S. Ratynskaia, K. Rypdal, C. Knapek, S. Khrapak, A. V. Milovanov, A. Ivlev, J. J. Rasmussen, and G. E. Morfill, *Phys. Rev. Lett.* **96**, 105010 (2006).
- [13] C. L. Chan and L. I., *Phys. Rev. Lett.* **98**, 105002 (2007).
- [14] G. J. Kalman, P. Hartmann, Z. Donkó, and M. Rosenberg, *Phys. Rev. Lett.* **92**, 065001 (2004).
- [15] S. Ichimaru, *Rev. Mod. Phys.* **54**, 1017 (1982).
- [16] T. Ott and M. Bonitz, *Phys. Rev. Lett.* **103**, 195001 (2009).
- [17] H. Ohta and S. Hamaguchi, *Phys. Plasmas* **7**, 4506 (2000).
- [18] Z. Donkó, J. Goree, and P. Hartmann, *Phys. Rev. E* **81**, 056404 (2010).
- [19] P. Hartmann, M. Cs. Sándor, A. Kovács, and Z. Donkó, *Phys. Rev. E* **84**, 016404 (2011).
- [20] S. Ratynskaia, G. Regnoli, B. Klumov, and K. Rypdal, *Phys. Plasmas* **17**, 034502 (2010).
- [21] T. Saigo and S. Hamaguchi, *Phys. Plasmas* **9**, 1210 (2002).
- [22] Z. Donkó, G. J. Kalman, and K. I. Golden, *Phys. Rev. Lett.* **88**, 225001 (2002).
- [23] J. Daligault, *Phys. Rev. Lett.* **96**, 065003 (2006).
- [24] Y. Feng, J. Goree, and B. Liu, *Phys. Rev. E* **82**, 036403 (2010).
- [25] D. J. Evans, *Phys. Rev. A* **23**, 2622 (1981).
- [26] U. Balucani, J. P. Brodholt, P. Jedlovsky, and R. Vallauri, *Phys. Rev. E* **62**, 2971 (2000).
- [27] T. R. Kirkpatrick, *Phys. Rev. Lett.* **53**, 1735 (1984).
- [28] M. S. Murillo, *Phys. Rev. Lett.* **85**, 2514 (2000).
- [29] D. Bertolini and A. Tani, *Phys. Rev. E* **51**, 1091 (1995).
- [30] J.-P. Hansen and I. R. McDonald, *Theory of Simple Liquids*, 2nd ed. (Elsevier, London, 1986).
- [31] J. P. Mithen, J. Daligault, and G. Gregori, *Contrib. Plasma Phys.* **52**, 58 (2012).